



1 **An Overlooked Kinetic Relaxation in the Formation of Sesquiterpene-Derived**
2 **Criegee Intermediates**

3

4 Hengjia Ou,^{1,†} Yao Li,^{2,†} Yuqing Sha,³ Hui Zhou,^{4,5} Jingkun Jiang,⁶ Kunpeng Chen^{4,6,*}

5

6 ¹Guangzhou Institute of Tropical and Marine Meteorology of China Meteorological
7 Administration, Guangzhou 510640, China

8 ²Yantai Meteorological Bureau, Yantai, Shandong 264003, China

9 ³Fuyang Meteorological Bureau, Fuyang, Anhui 236000, China

10 ⁴Key Laboratory for Thermal Science and Power Engineering of Ministry of Education, Beijing
11 Key Laboratory of CO₂ Utilization and Reduction Technology, Department of Energy and Power
12 Engineering, Tsinghua University, Beijing 100084, China

13 ⁵Shanxi Research Institute for Clean Energy, Tsinghua University, Shanxi, Taiyuan 030000, China

14 ⁶State Key Laboratory of Regional Environment and Sustainability, School of Environment,
15 Tsinghua University, Beijing 100084, China

16

17 Email: chenkp@mail.tsinghua.edu.cn

18

19 [†]Hengjia Ou and Yao Li contributed equally to this work.

20



21 **Abstract**

22 Criegee intermediates (CIs) from sesquiterpene ozonolysis contribute to secondary organic aerosol
23 (SOA) formation. The ozonolysis rate constants of typical sesquiterpenes have been measured by
24 prior experiments, but whether these values can represent the formation rate constants of
25 sesquiterpene-derived CIs remains questionable. This study reports the overlooked kinetic
26 relaxation in the CI formation from representative sesquiterpenes, including α -cedrene, α -copaene,
27 β -caryophyllene, α -farnesene and β -farnesene. We found that the apparent formation rate constant
28 of sesquiterpene-derived CIs is initially unstable but gradually approaches a plateau, which equals
29 the rate constant of sesquiterpene ozonolysis. Such behavior arises because CI formation cannot
30 instantaneously respond to sesquiterpene ozonolysis due to the finite time for the production of
31 primary ozonides (POZs). Our results also reveal that the kinetic relaxation is sensitive to
32 temperature variations, as cold surges extend the relaxation timescale from minutes to hours (or
33 hours to days) for most sesquiterpenes while heatwaves reversely diminish the relaxation
34 timescale. Exceptionally, β -caryophyllene exhibits the longest relaxation timescale (at least 2.6
35 days) even during the heatwaves. Our findings demonstrate that neglecting this kinetic relaxation
36 may substantially overestimate the rate of sesquiterpene-derived CI formation and thus the CI-
37 driven atmospheric oxidation capacity under extreme temperature conditions.

38

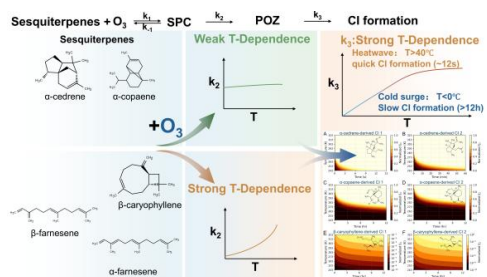
39 **Keywords**

40 ozone, volatile organic compounds, primary ozonide, relaxation, extreme temperature

41



42 TOC



43



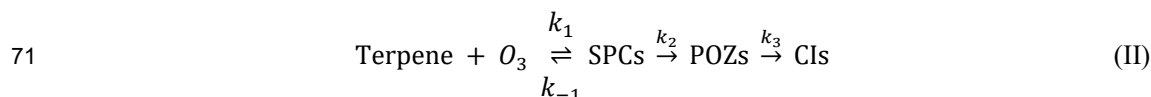
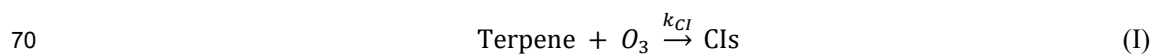
44 1. Introduction

45 Atmospheric Criegee intermediates (CIs) are produced from the ozonolysis of airborne
46 alkenes such as terpenes (Criegee, 1975; Johnson and Marston, 2008), but whether the formation
47 rate of CIs equals the rate of ozonolysis is still a question. The formation of CIs from reactions
48 between terpenes and ozone (O_3) contributes to the atmospheric oxidation capacity (Khan et al.,
49 2018; Chhantyal-Pun et al., 2020), which governs the formation of O_3 -initiated secondary organic
50 aerosols (SOAs) (Zhao et al., 2015; Zhao et al., 2016; Gong and Chen, 2021). CI chemistry
51 produces hydroxyl radicals and organic hydroperoxides (ROOHs) (Docherty et al., 2005; Reinnig
52 et al., 2009; Donahue et al., 2011; Iyer et al., 2021), which further boost the formation of
53 oxygenated species (e.g., carbonyls, alcohols) with high molecular weights in SOAs
54 (Dekermenjian et al., 1999; Jaoui et al., 2003; Jaoui et al., 2004; Kanawati et al., 2008; Reinnig et
55 al., 2009; Jaoui et al., 2013; Jaoui et al., 2017). The formation rate of CIs is determined not only
56 by the concentrations of O_3 and terpenes but also by the formation rate constant (k_{CI}). The value
57 of k_{CI} is always assumed equal to the ozonolysis rate constant (k_{oz}) in the literature (Taatjes et al.,
58 2014; Cox et al., 2020).

59 However, k_{CI} and k_{oz} are not necessarily interchangeable. In principle, terpene ozonolysis
60 directly produces stabilized prereactive complexes (SPCs) and subsequently primary ozonides
61 (POZs), which further decompose into CIs (Donahue et al., 2011; Vereecken and Francisco, 2012;
62 Taatjes et al., 2014). By definition, k_{CI} refers to the projection from the reactants (i.e., terpenes and
63 O_3) to CIs (Scheme I), but k_{oz} refers to the projection from the reactants to POZs (Scheme II) (Ou
64 and Chen, 2025; Ou et al., 2026), so there is no guarantee that k_{CI} can be equal to k_{oz} . Even if k_{CI}
65 equals k_{oz} at some temperatures, k_{oz} is analytically expressed as a function of k_1 , k_{-1} and k_2 (Ou and
66 Chen, 2025; Ou et al., 2026), whereas k_{CI} is not only related to k_1 , k_{-1} and k_2 but also k_3 . Since k_1 ,
67 k_{-1} , k_2 , and k_3 possess their own temperature dependence, k_{CI} may exhibit a more complicated



68 response to temperature variations compared to k_{oz} . To date, the field lacks a kinetically rigorous
69 framework for resolving the rate constants of CI formation.



72 This study discloses a previously unrecognized phenomenon, termed “kinetic relaxation”,
73 by explicitly elucidating the relationship between k_{CI} and k_{oz} . Kinetic relaxation refers to a transient
74 deviation of k_{CI} from k_{oz} . We chose CIs from sesquiterpene ozonolysis as the study case because
75 (1) the rate constants of sesquiterpene ozonolysis mostly show no dependence on air pressure in
76 the troposphere, and (2) the large molecular size of sesquiterpenes renders SPCs and POZs
77 collisionally stable (Wong et al., 2003; Yao et al., 2017; Ou and Chen, 2025). The sesquiterpene-
78 derived CIs thus serve as a simplified system that maintains a clear “double-well” potential energy
79 surface along the CI formation mechanism (Donahue et al., 2011; Vereecken and Francisco, 2012;
80 Taatjes et al., 2014), which is key to understanding the kinetic relaxation. The studied
81 sesquiterpenes involve α -cedrene, α -copaene, β -caryophyllene, α -farnesene and β -farnesene,
82 which are representative in the troposphere and emitted from vegetation in forests and farms
83 (Lwande et al., 1989; Arey et al., 1995; Duhl et al., 2008; Yee et al., 2018; Frazier et al., 2022;
84 Chen et al., 2024). Ozonolysis represents the predominant fate of these compounds (Shu and
85 Atkinson, 1995; Richters et al., 2015; Frazier et al., 2022), and most of their CIs (e.g., ~88% for
86 α -cedrene and >60% for β -caryophyllene) can be stabilized in the atmosphere (Winterhalter et al.,
87 2009; Nguyen et al., 2009; Yao et al., 2014). We estimated all the kinetic parameters with a
88 computational approach that can replicate the temperature-dependent ozonolysis rate constants of
89 α -cedrene (Fig. S1 in the supporting information) and β -caryophyllene (Ou and Chen, 2025). The



90 influence of temperature variations on sesquiterpene ozonolysis kinetics as well as the relaxation
91 timescale is also explored. The atmospheric implications of kinetic relaxation in the sesquiterpene-
92 derived CI formation kinetics are further discussed.

93 2. Methods

94 2.1 Kinetics of Sesquiterpene Ozonolysis

95 The rate constant of sesquiterpene ozonolysis (k_{oz}) can be expressed by Eq. (1), as presented
96 in our previous studies (Ou and Chen, 2025; Ou et al., 2026).

$$97 \quad k_{oz} = k_1 \cdot \sum_i \left[p_i \cdot \left(\frac{k_{2,i}}{k_{-1,i} + k_{2,i}} \right) \right] \quad (1)$$

98 Here k_l is the bimolecular collision rate constant of the sesquiterpene molecule and O₃,
99 which is calculated by the collision theory; p_i is the branching ratio of the i -th SPC arisen from the
100 bimolecular collisions, which is also corresponding to the i -th POZ; $k_{-1,i}$ and $k_{2,i}$ are the rate
101 constants of the backward dissociation of the i -th SPC and the forward formation of the i -th POZ,
102 respectively. All these quantities can be affected by temperature variations, and the ratio $k_{2,i} / (k_{-1,i}$
103 $+ k_{2,i})$ serves as the main factor to control the temperature dependence of the i -th POZ formation
104 kinetics (Ou and Chen, 2025). Since the temperature-dependent ozonolysis rate constants of β -
105 caryophyllene, α -farnesene and β -farnesene have been quantified by previous experimental
106 measurements (Kim et al., 2011; Gao et al., 2022), Eq. (1) was employed to estimate the
107 temperature-dependent ozonolysis rate constants of α -cedrene and α -copaene.

108 2.2 Kinetics of CI Formation

109 The computation of k_{CI} is based on the steady-state concentration of SPCs (Text S1), which
110 is supported by experimental measurements (Talukdar et al., 2003; Davis et al., 2005; Ou and
111 Chen, 2025). The expression of k_{CI} is approximated by Eq. (2), wherein $f_{CI,i}$ is the projection factor
112 for the i -th CI, as given by Eq. (3), if the initial concentrations of all POZs are zero.



113
$$k_{CI} \approx k_{oz} \cdot \sum_i f_{CI,i} \quad (2)$$

114
$$f_{CI,i} = r_i \cdot (1 - e^{-k_{3,i} \cdot t}) \quad (3)$$

115 In Eq. (3), t is time after ozonolysis starts, r_i is the steady-state branching ratio of the i -th
116 CI formation, which satisfies $\sum_i r_i = 1$ (Text S1), and $k_{3,i}$ is the rate constant of the i -th CI formation
117 from POZ decomposition. When the initial concentrations of POZs are not zero, $f_{CI,i}$ should be
118 implemented with a scale factor s_i (Text S2). Eq. (3) also shows that, when t equals 0, $f_{CI,i}$ also
119 equals 0 (Text S1); if the i -th POZ pre-exists before the ozonolysis (i.e., s_i shows up in $f_{CI,i}$), the
120 value of $f_{CI,i}$ will equal $r_i \cdot s_i$ when t equals 0 (Text S2). Regardless of the s_i , if t is infinitely large,
121 $f_{CI,i}$ will equal 1 so that k_{CI} will converge with k_{oz} (Text S1 and S2). Eqs. (2) and (3) show that k_{CI}
122 is not equal to k_{oz} at the beginning of ozonolysis, but k_{CI} approaches k_{oz} after a period of relaxation.
123 The projection factors $f_{CI,i}$ represent the kinetic relaxation of each CI generated from sesquiterpene
124 ozonolysis.

125 **2.3 Thermodynamic and Kinetic Computation**

126 The thermodynamic parameters such as zero-point energy (ZPE) and vibrational
127 frequencies were computed by the ORCA 5.0.4 software (Neese, 2012). Vibrational analysis based
128 on the optimized structures was conducted by the density functional theory (DFT) with the M06-
129 2X functional (Zhao and Truhlar, 2008) and the def2-TZVP basis set (Weigend and Ahlrichs,
130 2005). The RIJCOSX approximation was also employed to accelerate all the calculations (Neese
131 et al., 2009). Single-point energy was computed by using the DLPNO-CCSD(T) method with the
132 def2-TZVPP basis set (Riplinger and Neese, 2013; Weigend and Ahlrichs, 2005), accelerated by
133 the RIJCOSX algorithm as well. For benchmarking, the same DLPNO-CCSD(T) method was also
134 applied with the cc-pVTZ basis set (Dunning, 1989; Weigend et al., 2002), and the resulting energy
135 barriers were 0.3–0.5 kcal mol⁻¹ higher than those obtained by using def2-TZVPP (Table S4). The



136 thermodynamic parameters were used to calculate p_i , $k_{-1,i}$, $k_{2,i}$, and $k_{3,i,j}$ within the temperature
137 range of 243–323 K and the temperature increment of 5 K using the J-resolved microcanonical
138 variational transition state theory (mVTST) incorporated in the Multiwell 2023 program (Barker,
139 2009, 2001). Detailed computation procedures and accuracy tests were described in our previous
140 study (Ou and Chen, 2025).

141 **2.4 Arrhenius Fitting of Temperature Dependence**

142 The computed $k_{-1,i}$, $k_{2,i}$, and $k_{3,i,j}$ were further fitted by the Arrhenius equation $k(T) = A \cdot$
143 $\exp(-E_a / (RT))$, wherein A is the pre-exponential factor, E_a is the activation energy, and R is the
144 ideal gas constant. The temperature dependence of $k_{-1,i}$, $k_{2,i}$, and $k_{3,i,j}$ is controlled by the value of
145 E_a . The computed k_{oz} was fitted by the modified Arrhenius equation (Eq. (4)).

$$146 \quad k_{oz} \approx F_{oz} \cdot \left(\frac{T}{298}\right)^m \cdot e^{\Theta/T} \quad (4)$$

147 Here F_{oz} is the temperature-independent constant for ozonolysis, m is the constant for
148 temperature dependence of the power-law factor, and Θ is the constant for temperature dependence
149 of the exponential factor.

150 **3. Results and Discussions**

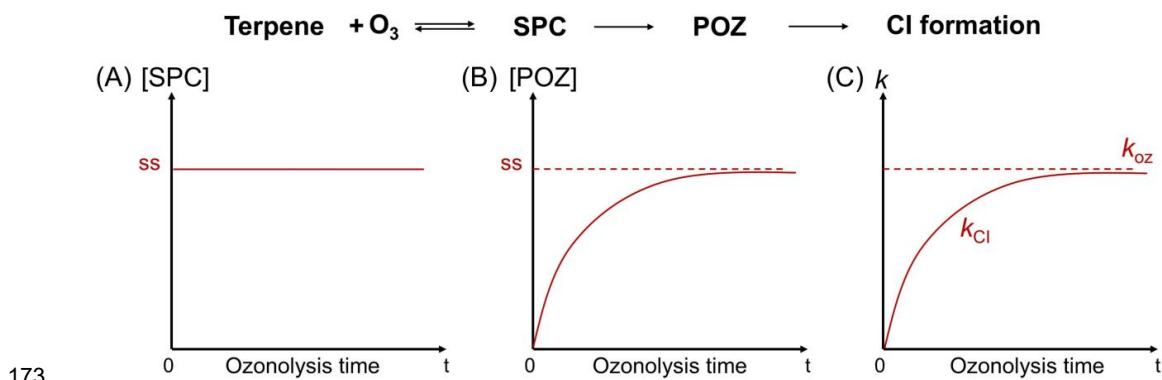
151 **3.1 The Origin of Kinetic Relaxation**

152 The kinetic relaxation was found when we opened the "black box" kinetic model of CI
153 formation. The rate constant for CI formation is assumed equal to that of ozonolysis, as previously
154 suggested (Taatjes et al., 2014; Cox et al., 2020). Such assumption treats the processes from
155 sesquiterpene ozonolysis to CI formation as a "black box" in which inflow and outflow are
156 considered balanced. As we open the kinetic model, SPCs and POZs lay inside and a more reliable
157 foundation comes up, which is to assume the steady-state SPC concentrations (Fig. 1A). This is an
158 assumption consolidated by the experimental measurements of temperature-dependent kinetics



159 (Talukdar et al., 2003; Davis et al., 2005; Ou and Chen, 2025). Under the steady-state SPC
 160 concentrations, we find that the concentrations of POZs are time-dependent (Text S1). The
 161 concentration of each POZ is initially zero, subsequently increases along with ozonolysis time,
 162 and asymptotically approaches a plateau value that represents the steady-state POZ concentration
 163 (Fig. 1B).

164 The time-dependent concentration of POZs causes k_{CI} to also vary with time (Text S1). The
 165 well-established mechanism of CI formation indicates that CIs are not directly generated from the
 166 reactive collision between alkenes and O_3 but from the decomposition of POZs (Criegee, 1975;
 167 Donahue et al., 2011; Taatjes et al., 2014; Vereecken and Francisco, 2012). So, in principle, k_{CI} is
 168 in principle proportional to the POZ concentration. At the beginning of ozonolysis, k_{CI} is also zero
 169 unless pre-existing POZs are present before the ozonolysis (Text S2). The value of k_{CI} increases
 170 over time and asymptotically approaches its plateau value (Fig. 1C), which is exactly k_{oz} (Text S1).
 171 Our deductive results suggest that only when both SPCs and POZs are at their steady-state
 172 concentrations can k_{CI} be equal to k_{oz} .



174 **Figure 1.** The origin of kinetic relaxation of CI formation: (A) steady-state (ss) SPC concentration;
 175 (B) time-dependent POZ concentration; (C) time-dependent CI formation rate constant (k_{CI}),
 176 which ultimately reaches a stable value equal to the ozonolysis rate constant (k_{oz}).
 177

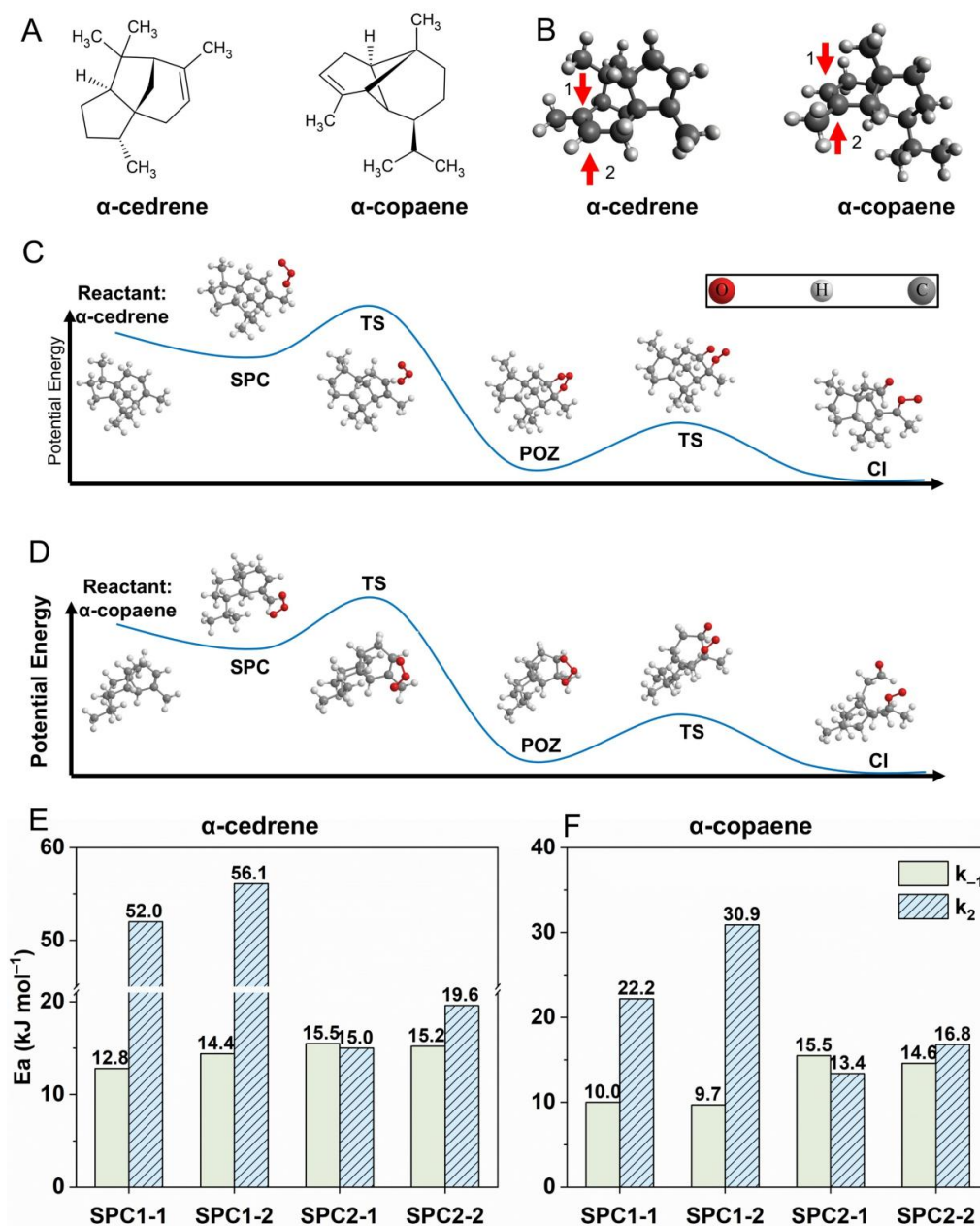


178 3.2 Competition Between SPC Dissociation and POZ Production

179 The kinetic relaxation of CI formation is based on the steady-state concentrations of SPCs,
180 which is balanced by the kinetic competition between SPC dissociation (k_{-1}) and POZ production
181 (k_2). The POZ production tendency is quantified by the ratio $k_2 / (k_{-1} + k_2)$ (Fig. S2 and S3), and
182 the comparisons of activation energies ($E_a(k_{-1})$ and $E_a(k_2)$) from the Arrhenius fitting can help a
183 clear analysis of temperature dependence (Fig. 2E and 2F, Table S1).

184 Taking α -cedrene and α -copaene as examples, both molecules have only one C=C double
185 bond (Fig. 2A), and both have two sites for ozonolysis (Fig. 2B). Since each POZ has two
186 conformers (Ou and Chen, 2025; Ou et al., 2026), there are totally four POZs can be formed for
187 α -cedrene or α -copaene (Fig. S4). For α -cedrene, site 2 dominates POZ production with the
188 branching ratio at SPC2-1 of >89% (Table S2). The values of $E_a(k_2)$ and $E_a(k_{-1})$ are comparable at
189 site 2, with SPC2-1 uniquely showing $E_a(k_2) < E_a(k_{-1})$ (Fig. 2E). The resultant $k_2 / (k_{-1} + k_2)$ shows
190 different temperature dependence for SPC2-1 and SPC2-2 (Fig. S2C and 2D), with the case in
191 SPC2-1 remaining largely stable across temperatures. Similarly, POZ production from α -copaene
192 exclusively occurs at site 2, with the SPC2-1: SPC2-2 branching ratio of ~3:1 at 243 K and ~3:2
193 at 323 K (Table S2). The ratio $k_2 / (k_{-1} + k_2)$ at site 2 does not decrease significantly with declining
194 temperature (Fig. S3C and S3D).

195 Our findings reveal that, if $E_a(k_2)$ is higher than $E_a(k_{-1})$, SPC dissociation is favored so that
196 ozonolysis through this SPC is infeasible. Conversely, if $E_a(k_2)$ is lower than $E_a(k_{-1})$, POZ
197 formation is feasible and the associated ozonolysis channel is highly efficient. Since branching
198 ratios of all the SPCs minorly vary with temperature (Table S2), the ozonolysis channels of α -
199 cedrene and α -copaene are very stable across a wide temperature range. Such a robust ozonolysis
200 mechanism directly identifies representative POZs responsible for further CI formation.



201 **Figure 2.** Examples of sesquiterpene ozonolysis kinetics: (A) Molecular structures of α -cedrene
 202 and α -copaene; (B) ozonolysis site 1 and 2 labelled on the molecular structures; the “double-well”
 203 potential energy surface of the formation of (C) an example of α -cedrene-derived CI and (D) an
 204 example of α -copaene-derived CI; fitted activation energies of k_{-1} and k_2 among the ozonolysis
 205 SPCs of (E) α -cedrene and (F) α -copaene.
 206
 207



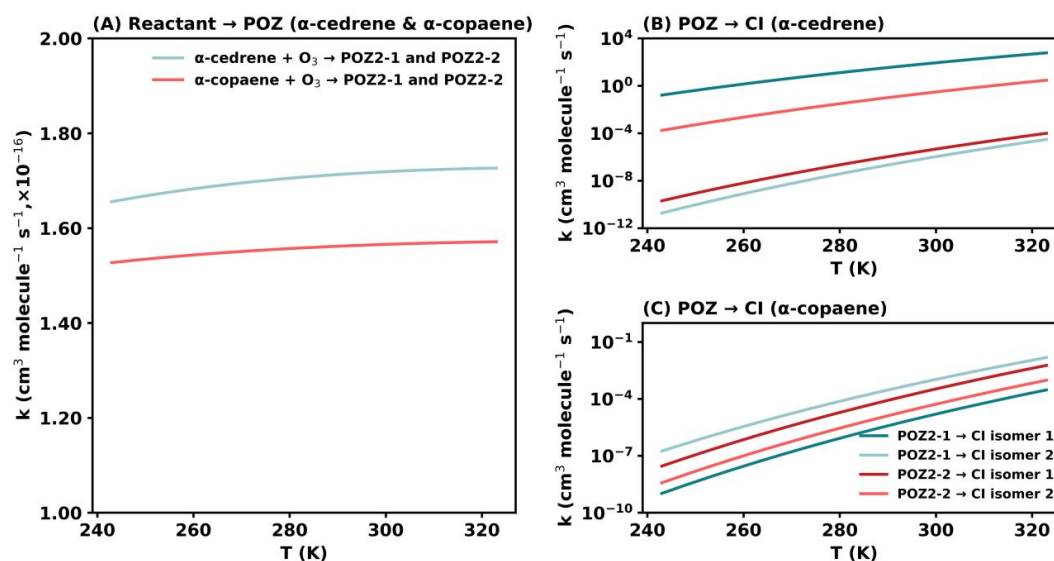
208 3.3 Temperature-Dependent Kinetics of Ozonolysis and POZ Decomposition

209 The kinetic competition between SPCs and POZs only affects the value of k_{oz} , while the
210 value of k_{CI} not only depends on k_{oz} but also the decomposition rate constant of POZs (k_3). Here
211 we examine the temperature-dependent ozonolysis kinetics of the studied sesquiterpenes, with
212 particular attention to the anomalous behavior of α -cedrene and α -copaene. The ozonolysis kinetics
213 of α -cedrene and α -copaene exhibit only weak temperature dependence (Fig. 3A). Despite the wide
214 temperature range, their k_{oz} remain within a narrow interval ($\sim 1.5\text{--}1.7 \times 10^{-16} \text{ cm}^3 \text{ molecule}^{-1} \text{ s}^{-1}$).
215 The analytical fitting based on the modified Arrhenius equation gives $k_{oz} = 3.8 \times 10^{-16} \times (T /$
216 $298)^{-0.7} \times \exp(-236.6 / T)$ for α -cedrene and $k_{oz} = 2.5 \times 10^{-16} \times (T / 298)^{-0.4} \times \exp(-139.6 / T)$ for
217 α -copaene (Fig. S5). In these expressions, the exponential terms increase with temperature,
218 whereas the temperature-dependent pre-exponential factors decrease (Fig. S6). This phenomenon
219 is different from those of β -caryophyllene and farnesenes, wherein β -caryophyllene exhibits an
220 increasing exponential factor as temperature increases, while farnesenes show decreasing
221 exponential factors (Fig. S6) (Kim et al., 2011; Gao et al., 2022). Notably, their pre-exponential
222 factors remain unchanged along with the temperature variations, in contrast to the compensating
223 trends observed for α -cedrene and α -copaene (Fig. S6). Among the studied sesquiterpenes, α -
224 cedrene and α -copaene are very resistant to temperature variations regarding their k_{oz} values. The
225 resistant k_{oz} indicates that the POZ production flux is correspondingly stable.

226 Unlike the weak temperature dependence of k_{oz} for α -cedrene and α -copaene, their POZ
227 decomposition kinetics (represented by k_3) show a much more dramatic response to temperature.
228 The value of k_3 increases by 3–6 orders of magnitude as the temperature increases from 243 to 313
229 K (Fig. 3B and 3C). Although each POZ can decompose via two channels to form two CI isomers,
230 our results reveal that only one pathway clearly dominates. For α -cedrene, POZ2-1 mainly
231 produces its CI isomer 1, while POZ2-2 mainly produces its CI isomer 2 (Fig. 3B). For α -copaene,



232 POZ2-1 favors the formation of its CI isomer 2 whereas POZ2-2 favors the formation of its CI
 233 isomer 1 (Fig. 3C). For each POZ, the rate constant for producing the predominant CI consistently
 234 exceeds that of the other CI at every temperature within 243–323 K by multiple orders of
 235 magnitude.



236
 237 **Figure 3.** Temperature dependence of (A) ozonolysis rate constants (k_{oz}) of α -cedrene and α -
 238 copaene, and POZ decomposition rate constants (k_3) for (B) α -cedrene-derived CIs and (C) α -
 239 copaene-derived CIs.

240
 241 The strong temperature dependence arises from the high activation energies associated with
 242 POZ decomposition (Fig. S7). Once formed, sesquiterpene-derived POZs rapidly stabilize by
 243 colliding with the surrounding gas molecules (Chuong et al., 2004; Hakala and Donahue, 2023),
 244 mainly nitrogen and oxygen in the air, which inhibits rapid decomposition. The level of collisional
 245 stabilization may also depend on air pressure, so that the value of k_3 could potentially show
 246 pressure dependence. Nevertheless, our findings reveal that the formation kinetics of
 247 sesquiterpene-derived CIs are far more sensitive to temperature variations than the sesquiterpene
 248 ozonolysis kinetics.



249 3.4 Relaxation Timescale of CI Formation

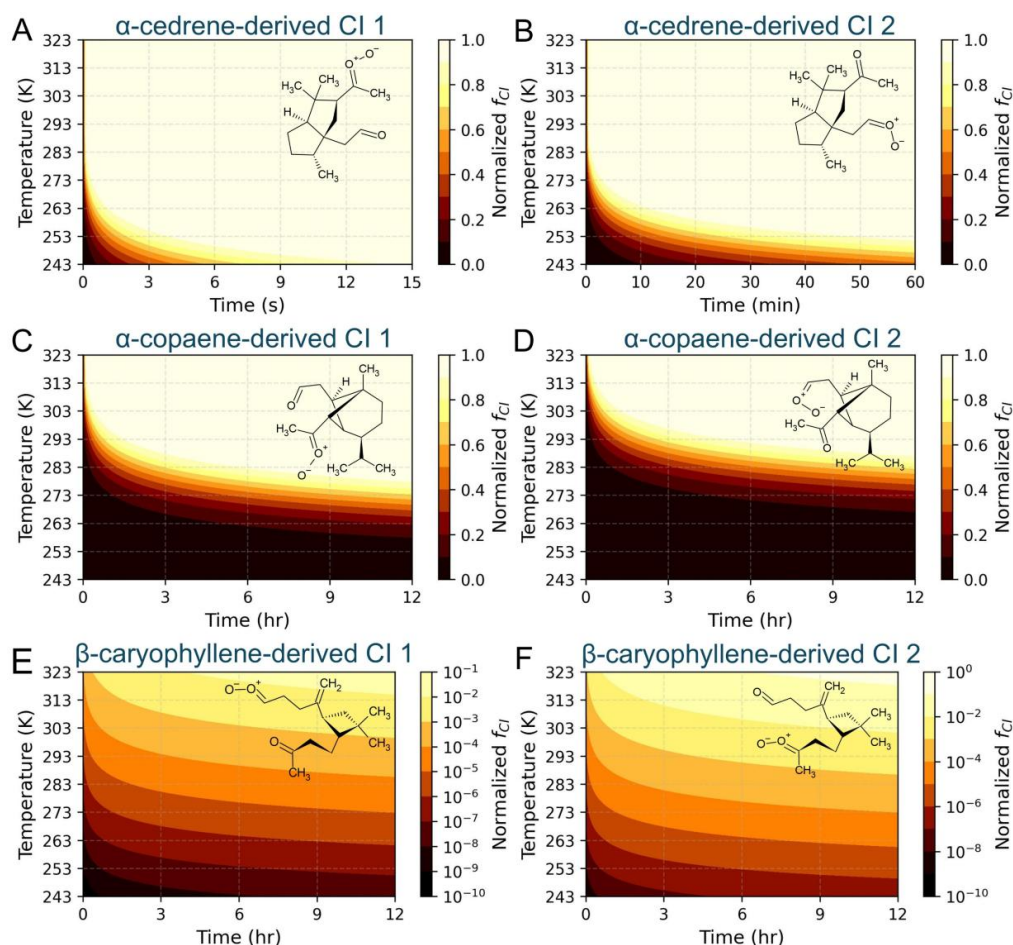
250 We further explore the temperature-dependent relaxation of CI formation kinetics. The
251 kinetic relaxation at different temperatures can be visualized by the contour of “normalized f_{CI} ”
252 (i.e., $f_{CI,i} / r_i$ as referred to Eq. (2)) (Fig. 4), and the relaxation timescale is estimated by $1 / k_3$
253 (Tables 1 and S3). Taking α -cedrene as an example, the normalized f_{CI} for CI isomer 1 reaches
254 unity in less than 1 s at temperatures above 273 K, while it approaches unity within 6 s at 243 K
255 (Fig. 4A). The relaxation timescale is within 0.1 minutes at the studied temperatures (Table 1). In
256 contrast, for α -cedrene-derived CI isomer 2, the normalized f_{CI} reaches unity in ~ 1 min at
257 temperatures above 273 K but requires more than 1 hour at 243 K (Fig. 4B). The relaxation
258 timescale is negligibly short at 323 K but extended to 96.9 minutes at 243 K (Table 1). These
259 results reveal that different CIs derived from the same sesquiterpene may exhibit divergent
260 relaxation timescales.

261 If the relaxation timescale extends to half a day or even longer, kinetic relaxation will
262 considerably reduce the formation rate constants of CIs. Taking α -copaene as an example, when
263 the temperature falls below 273 K, the relaxation timescales are over 10 hours and 40 hours for its
264 CI1 and CI2, respectively (Table 1). The normalized f_{CI} is below 0.1 for more than 1 hour, meaning
265 that the formation rate constants for both CIs are less than 10% of their steady-state values for a
266 non-negligible timescale (Fig. 4C and 4D). However, during heatwaves over 313 K, the relaxation
267 timescales are hugely reduced to less than 10 minutes (Table 1). These findings reveal that
268 heatwaves can diminish kinetic relaxation to a negligible level for the α -copaene-derived CIs.

269 Moreover, an identical CI may be produced from structurally similar sesquiterpenes, but
270 the relaxation timescales are different. Taking α -farnesene and β -farnesene as examples, their
271 ozonolysis proceeds predominantly from the same C=C double bonds (Kourtchev et al., 2009;



272 Jaoui et al., 2017), yielding the same CI (CI1 in Fig. S8A and S8C). During cold surges at 243 K,
 273 the relaxation timescale in α -farnesene ozonolysis is 3 orders of magnitude larger than that in β -
 274 farnesene ozonolysis, but during heatwaves, the CI1 from both farnesenes has a negligible
 275 relaxation timescale (Table S3). The dramatic decrease in relaxation timescale also holds for other
 276 CIs generated from α -farnesene and β -farnesene (Fig. S8B and S8D). Our results suggest that
 277 kinetic relaxation may be more general during cold surges.



278
 279 **Figure 4.** Kinetic relaxation of the temperature-dependent formation rate constant of (A) α -
 280 cedrene-derived CI isomer 1; (B) α -cedrene-derived CI isomer 2; (C) α -copaene-derived CI isomer
 281 1; (D) α -copaene-derived CI isomer 2; (E) β -caryophyllene-derived CI isomer 1; (F) β -
 282 caryophyllene-derived CI isomer 2.
 283



284 **Table 1.** Relaxation timescale of CI formation from the ozonolysis of α -cedrene, α -copaene, and
 285 β -caryophyllene.

T (K)	α -cedrene (unit: minutes)		α -copaene (unit: hours)		β -caryophyllene (unit: days)	
	CI1	CI2	CI1	CI2	CI1	CI2
243	0.1	96.9	1576.1	9791.6	2.8×10^7	2.1×10^6
248	0.1	44.0	628.5	3635.0	9.0×10^6	6.8×10^5
253	0.0	20.6	259.7	1402.5	2.9×10^6	2.4×10^5
258	0.0	9.9	111.0	561.1	9.7×10^5	8.3×10^4
263	0.0	4.9	49.0	232.3	3.5×10^5	3.2×10^4
268	0.0	2.5	22.3	99.4	1.3×10^5	1.3×10^4
273	0.0	1.3	10.4	43.8	4.9×10^4	5000.0
278	0.0	0.7	5.0	19.9	1.9×10^4	2083.3
283	0.0	0.4	2.5	9.3	7638.9	902.8
288	0.0	0.2	1.2	4.4	3263.9	388.9
293	0.0	0.1	0.6	2.2	1388.9	180.6
298	0.0	0.1	0.3	1.1	631.9	83.3
303	0.0	0.0	0.2	0.6	284.7	39.6
308	0.0	0.0	0.1	0.3	131.9	19.4
313	0.0	0.0	0.06	0.2	64.6	9.7
318	0.0	0.0	0.03	0.1	31.9	4.9
323	0.0	0.0	0.02	0.05	16.0	2.6

286

287 Surprisingly, β -caryophyllene-derived CIs show substantial kinetic relaxation regardless
 288 of the temperature variations (Fig. 4E and 4F). Across the entire temperature range, the normalized
 289 f_{CI} remains 1–10 orders of magnitude lower than unity, showing much stronger temperature
 290 dependence driven by the high activation energies of k_3 (Fig. S7). Even under the heatwaves at
 291 323 K, the relaxation timescales are at least 2.6 days (Table 1). It is again highlighted that the
 292 calculated values of k_3 as well as the relaxation timescale are based on entirely collisional
 293 stabilization of POZs. In the real atmosphere, as air pressure changes spatiotemporally, different
 294 levels of incomplete collisional stabilization may occur, such that the value of k_3 could be higher



295 and the relaxation timescale correspondingly shorter. Even so, β -caryophyllene still has the longest
296 relaxation timescales among the studied sesquiterpenes. Neglecting such prolonged relaxation may
297 systematically overestimate the formation rate of β -caryophyllene-derived CIs.

298 It is also noted that our results above are based on simplified cases where the pre-existing
299 POZs are absent. Our supplemental simulations with the POZ scale factors show that the value of
300 normalized f_{CI} can be amplified but the relaxation timescales remain almost unchanged (Fig. S9).
301 Our findings collectively demonstrate that relaxation timescales and their response to temperature
302 variation can be highly distinct for different sesquiterpenes. Relaxation may be negligible in long-
303 term modeling studies for most sesquiterpenes during heatwaves, but it may still be a great concern
304 in cold surge simulations.

305 **4. Conclusions**

306 Kinetic relaxation is a previously unrecognized behavior in the formation of CIs from
307 sesquiterpene ozonolysis. This relaxation arises from the finite time for POZ production, which
308 hinders an instantaneous response of CI formation to sesquiterpene ozonolysis. The relaxation
309 timescale is sensitive to temperature variations and may be amplified during cold surges and
310 suppressed during heatwaves. Under future warming scenarios (Perkins-Kirkpatrick and Lewis,
311 2020; Martinez-Villalobos et al., 2025) as well as less frequent cold surges (Nie et al., 2025;
312 Blackport and Fyfe, 2024), kinetic relaxation could become less important on average, although
313 substantial regional and seasonal variability is expected. It is also worth noting that the global trend
314 does not necessarily represent spatiotemporal variations of temperatures; the low temperatures at
315 high latitudes and intense cooling at night may still be possible to induce considerable kinetic
316 relaxation. Under such conditions, ignoring kinetic relaxation may lead to overestimation of CI



317 concentrations and therefore potentially overestimate the oxidation rates of trace gases such as SO₂
318 and NO₂ (Welz et al., 2012; Mauldin Iii et al., 2012; Chhantyal-Pun et al., 2020).
319 This study also provides an additional perspective for estimating the impact of temperature
320 variation on SOA formation. CI chemistry can contribute to SOA formation through the production
321 of highly oxygenated organic molecules (HOMs) with extremely low volatility (Zhao et al., 2015;
322 Richters et al., 2016a; Richters et al., 2016b). The rate of HOMs formation from sesquiterpene
323 ozonolysis may be considerably affected by the CI formation kinetics. Temperature variations
324 could modulate the formation rate of HOMs by inducing different levels of kinetic relaxation in
325 CI formation. A more comprehensive analysis of SOA formation should integrate detailed reaction
326 mechanisms, temperature-dependent sesquiterpene emission factors, temperature-dependent gas-
327 particle partitioning, and potentially new particle formation events. Among these complex factors,
328 kinetic relaxation uniquely offers a new aspect on the CI supply flux. Overall, our study
329 demonstrates that kinetic relaxation should be considered in atmospheric chemistry models when
330 simulating CI chemistry under conditions characterized by strong temperature variability or low
331 temperatures.



332 **Acknowledgments**

333 The authors would like to acknowledge computational resources in Tsinghua University as well
334 as those inherited from the late Professor Jun Zhao. Jingkun Jiang acknowledges support from the
335 National Natural Science Foundation of China (22536004). Hengjia Ou acknowledges the funding
336 from the Key Innovation Team of Guangdong Meteorological Bureau (No. GRMCTD202506-
337 ZD06). Yao Li acknowledges the funding from Talent Recruitment Special Project of the
338 Shandong Meteorological Bureau (No. 2025SDRCYJ07).

339

340 **Author Contribution**

341 Hengjia Ou, Yao Li, and Kunpeng Chen contributed to conceptualization, computational
342 methodology, investigation, formal analysis, and visualization. Yuqing Sha and Kunpeng Chen
343 contributed to equation derivation. Kunpeng Chen supervised the study. Jingkun Jiang, Hengjia
344 Ou, and Yao Li contributed to funding acquisition. Hui Zhou, Hengjia Ou and Yao Li contributed
345 to computational resources. Hengjia Ou, Yao Li, Yuqing Sha, and Kunpeng Chen contributed to
346 original draft writing. All authors contributed to draft review and editing.

347

348 **Data Availability**

349 All the data are available in the main text or the supplementary information.

350

351 **Competing Interest**

352 The authors declare no competing financial interest.

353



354 **References**

- 355 Arey, J., Crowley, D. E., Crowley, M., Resketo, M., and Lester, J.: Hydrocarbon emissions from
356 natural vegetation in California's South Coast Air Basin, *Atmos. Environ.*, 29, 2977-2988,
357 [https://doi.org/10.1016/1352-2310\(95\)00137-N](https://doi.org/10.1016/1352-2310(95)00137-N), 1995.
- 358 Barker, J. R.: Multiple-Well, multiple-path unimolecular reaction systems. I. MultiWell computer
359 program suite, *Int. J. Chem. Kinet.*, 33, 232-245, 10.1002/kin.1017, 2001.
- 360 Barker, J. R.: Energy transfer in master equation simulations: A new approach, *Int. J. Chem. Kinet.*,
361 41, 748-763, 10.1002/kin.20447, 2009.
- 362 Blackport, R. and Fyfe, J. C.: Amplified warming of North American cold extremes linked to
363 human-induced changes in temperature variability, *Nat. Commun.*, 15, 5864, 10.1038/s41467-024-
364 49734-8, 2024.
- 365 Chen, X., Gong, D., Liu, S., Meng, X., Li, Z., Lin, Y., Li, Q., Xu, R., Chen, S., Chang, Q., Ma, F.,
366 Ding, X., Deng, S., Zhang, C., Wang, H., and Wang, B.: In-situ online investigation of biogenic
367 volatile organic compounds emissions from tropical rainforests in Hainan, China, *Sci. Total*
368 *Environ.*, 954, 176668, <https://doi.org/10.1016/j.scitotenv.2024.176668>, 2024.
- 369 Chhantyal-Pun, R., Khan, M. A. H., Taatjes, C. A., Percival, C. J., Orr-Ewing, A. J., and Shallcross,
370 D. E.: Criegee intermediates: production, detection and reactivity, *Int. Rev. Phys. Chem.*, 39, 385-
371 424, 10.1080/0144235X.2020.1792104, 2020.
- 372 Chuong, B., Zhang, J., and Donahue, N. M.: Cycloalkene Ozonolysis: Collisionally Mediated
373 Mechanistic Branching, *J. Am. Chem. Soc.*, 126, 12363-12373, 10.1021/ja0485412, 2004.
- 374 Cox, R. A., Ammann, M., Crowley, J. N., Herrmann, H., Jenkin, M. E., McNeill, V. F., Mellouki,
375 A., Troe, J., and Wallington, T. J.: Evaluated kinetic and photochemical data for atmospheric



376 chemistry: Volume VII – Criegee intermediates, *Atmos. Chem. Phys.*, 20, 13497-13519,
377 10.5194/acp-20-13497-2020, 2020.

378 Criegee, R.: Mechanism of Ozonolysis, *Angew. Chem., Int. Ed.*, 14, 745-752,
379 <https://doi.org/10.1002/anie.197507451>, 1975.

380 Davis, M. E., Drake, W., Vimal, D., and Stevens, P. S.: Experimental and theoretical studies of the
381 kinetics of the reactions of OH and OD with acetone and acetone-d₆ at low pressure, *J. Photochem.*
382 *Photobiol. A Chem.*, 176, 162-171, <https://doi.org/10.1016/j.jphotochem.2005.08.030>, 2005.

383 Dekermenjian, M., Allen, D. T., Atkinson, R., and Arey, J.: FTIR Analysis of Aerosol Formed in
384 the Ozone Oxidation of Sesquiterpenes, *Aerosol Sci. Technol.*, 30, 349-363,
385 10.1080/027868299304552, 1999.

386 Docherty, K. S., Wu, W., Lim, Y. B., and Ziemann, P. J.: Contributions of Organic Peroxides to
387 Secondary Aerosol Formed from Reactions of Monoterpenes with O₃, *Environ. Sci. Technol.*, 39,
388 4049-4059, 10.1021/es050228s, 2005.

389 Donahue, N. M., Drozd, G. T., Epstein, S. A., Presto, A. A., and Kroll, J. H.: Adventures in
390 ozoneland: down the rabbit-hole, *Phys. Chem. Chem. Phys.*, 13, 10848-10857,
391 10.1039/C0CP02564J, 2011.

392 Duhl, T. R., Helmig, D., and Guenther, A.: Sesquiterpene emissions from vegetation: a review,
393 *Biogeosciences*, 5, 761-777, 10.5194/bg-5-761-2008, 2008.

394 Dunning, T. H., Jr.: Gaussian basis sets for use in correlated molecular calculations. I. The atoms
395 boron through neon and hydrogen, *J. Chem. Phys.*, 90, 1007-1023, 10.1063/1.456153, 1989.

396 Frazier, G., McGlynn, D. F., Barry, L. E., Lerdau, M., Pusede, S. E., and Isaacman-VanWertz, G.:
397 Composition, concentration, and oxidant reactivity of sesquiterpenes in the southeastern U.S.,
398 *Environ. Sci. Atmos.*, 2, 1208-1220, 10.1039/D2EA00059H, 2022.



- 399 Gao, L., Song, J., Mohr, C., Huang, W., Vallon, M., Jiang, F., Leisner, T., and Saathoff, H.: Kinetics,
400 SOA yields, and chemical composition of secondary organic aerosol from β -caryophyllene
401 ozonolysis with and without nitrogen oxides between 213 and 313 K, *Atmos. Chem. Phys.*, 22,
402 6001-6020, 10.5194/acp-22-6001-2022, 2022.
- 403 Gong, Y. and Chen, Z.: Quantification of the role of stabilized Criegee intermediates in the
404 formation of aerosols in limonene ozonolysis, *Atmos. Chem. Phys.*, 21, 813-829, 10.5194/acp-21-
405 813-2021, 2021.
- 406 Hakala, J. and Donahue, N. M.: Carbonyl Oxide Stabilization from Trans Alkene and Terpene
407 Ozonolysis, *J. Phys. Chem. A*, 127, 8530-8543, 10.1021/acs.jpca.3c03650, 2023.
- 408 Iyer, S., Rissanen, M. P., Valiev, R., Barua, S., Krechmer, J. E., Thornton, J., Ehn, M., and Kurtén,
409 T.: Molecular mechanism for rapid autoxidation in α -pinene ozonolysis, *Nat. Commun.*, 12, 878,
410 10.1038/s41467-021-21172-w, 2021.
- 411 Jaoui, M., Leungsakul, S., and Kamens, R. M.: Gas and Particle Products Distribution from the
412 Reaction of β -Caryophyllene with Ozone, *J. Atmos. Chem.*, 45, 261-287,
413 10.1023/A:1024263430285, 2003.
- 414 Jaoui, M., Sexton, K. G., and Kamens, R. M.: Reaction of α -cedrene with ozone: mechanism, gas
415 and particulate products distribution, *Atmos. Environ.*, 38, 2709-2725,
416 <https://doi.org/10.1016/j.atmosenv.2004.02.007>, 2004.
- 417 Jaoui, M., Kleindienst, T. E., Docherty, K. S., Lewandowski, M., and Offenberg, J. H.: Secondary
418 organic aerosol formation from the oxidation of a series of sesquiterpenes: α -cedrene, β -
419 caryophyllene, α -humulene and α -farnesene with O₃, OH and NO₃ radicals, *Environ. Chem.*, 10,
420 178-193, 10.1071/EN13025, 2013.



- 421 Jaoui, M., Lewandowski, M., Offenberg, J. H., Docherty, K. S., and Kleindienst, T. E.: Ozonolysis
422 of α/β -farnesene mixture: Analysis of gas-phase and particulate reaction products, *Atmos. Environ.*,
423 169, 175-192, <https://doi.org/10.1016/j.atmosenv.2017.08.065>, 2017.
- 424 Johnson, D. and Marston, G.: The gas-phase ozonolysis of unsaturated volatile organic compounds
425 in the troposphere, *Chem. Soc. Rev.*, 37, 699-716, 10.1039/B704260B, 2008.
- 426 Kanawati, B., Herrmann, F., Joniec, S., Winterhalter, R., and Moortgat, G. K.: Mass spectrometric
427 characterization of β -caryophyllene ozonolysis products in the aerosol studied using an
428 electrospray triple quadrupole and time-of-flight analyzer hybrid system and density functional
429 theory, *Rapid Commun. Mass Spectrom.*, 22, 165-186, <https://doi.org/10.1002/rcm.3340>, 2008.
- 430 Khan, M. A. H., Percival, C. J., Caravan, R. L., Taatjes, C. A., and Shallcross, D. E.: Criegee
431 intermediates and their impacts on the troposphere, *Environ. Sci. Process. Impacts.*, 20, 437-453,
432 10.1039/C7EM00585G, 2018.
- 433 Kim, D., Stevens, P. S., and Hites, R. A.: Rate Constants for the Gas-Phase Reactions of OH and
434 O₃ with β -Ocimene, β -Myrcene, and α - and β -Farnesene as a Function of Temperature, *J. Phys.*
435 *Chem. A*, 115, 500-506, 10.1021/jp111173s, 2011.
- 436 Kourtchev, I., Bejan, I., Sodeau, J. R., and Wenger, J. C.: Gas-phase reaction of (E)- β -farnesene
437 with ozone: Rate coefficient and carbonyl products, *Atmos. Environ.*, 43, 3182-3190,
438 <https://doi.org/10.1016/j.atmosenv.2009.03.048>, 2009.
- 439 Lwande, W., McDowell, P. G., Amiani, H., and Amoke, P.: Analysis of airborne volatiles of cowpea,
440 *Phytochemistry*, 28, 421-423, [https://doi.org/10.1016/0031-9422\(89\)80025-1](https://doi.org/10.1016/0031-9422(89)80025-1), 1989.
- 441 Martinez-Villalobos, C., Fu, D., Loikith, P. C., and Neelin, J. D.: Accelerating increase in the
442 duration of heatwaves under global warming, *Nat. Geosci.*, 18, 716-723, 10.1038/s41561-025-
443 01737-w, 2025.



444 Mauldin Iii, R. L., Berndt, T., Sipilä, M., Paasonen, P., Petäjä, T., Kim, S., Kurtén, T., Stratmann,
445 F., Kerminen, V. M., and Kulmala, M.: A new atmospherically relevant oxidant of sulphur dioxide,
446 Nature, 488, 193-196, 10.1038/nature11278, 2012.

447 Neese, F.: The ORCA program system, Wires Comput Mol Sci, 2, 73-78, 10.1002/wcms.81, 2012.

448 Neese, F., Wennmohs, F., Hansen, A., and Becker, U.: Efficient, approximate and parallel Hartree–
449 Fock and hybrid DFT calculations. A ‘chain-of-spheres’ algorithm for the Hartree–Fock exchange,
450 Chem. Phys., 356, 98-109, <https://doi.org/10.1016/j.chemphys.2008.10.036>, 2009.

451 Nguyen, T. L., Winterhalter, R., Moortgat, G., Kanawati, B., Peeters, J., and Vereecken, L.: The
452 gas-phase ozonolysis of β -caryophyllene (C₁₅H₂₄). Part II: A theoretical study, Phys. Chem.
453 Chem. Phys., 11, 4173-4183, 10.1039/B817913A, 2009.

454 Nie, Y., Sun, Y., Zhang, X., and Chen, G.: Human-induced changes in extreme cold surges across
455 the Northern Hemisphere, Nat. Commun., 16, 8086, 10.1038/s41467-025-62576-2, 2025.

456 Ou, H. and Chen, K.: Atmospheric Temperature Dependence of β -Caryophyllene Ozonolysis
457 Kinetics Is Governed by Stabilized Prereactive Complexes, J. Phys. Chem. A, 129, 9982-9990,
458 10.1021/acs.jpca.5c05523, 2025.

459 Ou, H., Sha, Y., Deng, T., Zhou, H., and Chen, K.: Extreme Temperature Divergently Alters
460 Ozonolysis Kinetics of Atmospheric Cadinenes, ACS ES&T Air, 10.1021/acsestair.6c00017, 2026.

461 Perkins-Kirkpatrick, S. E. and Lewis, S. C.: Increasing trends in regional heatwaves, Nat.
462 Commun., 11, 3357, 10.1038/s41467-020-16970-7, 2020.

463 Reinnig, M.-C., Warnke, J., and Hoffmann, T.: Identification of organic hydroperoxides and
464 hydroperoxy acids in secondary organic aerosol formed during the ozonolysis of different
465 monoterpenes and sesquiterpenes by on-line analysis using atmospheric pressure chemical



466 ionization ion trap mass spectrometry, *Rapid Commun. Mass Spectrom.*, 23, 1735-1741,
467 <https://doi.org/10.1002/rcm.4065>, 2009.

468 Richters, S., Herrmann, H., and Berndt, T.: Gas-phase rate coefficients of the reaction of ozone
469 with four sesquiterpenes at 295 ± 2 K, *Phys. Chem. Chem. Phys.*, 17, 11658-11669,
470 10.1039/C4CP05542J, 2015.

471 Richters, S., Herrmann, H., and Berndt, T.: Different pathways of the formation of highly oxidized
472 multifunctional organic compounds (HOMs) from the gas-phase ozonolysis of β -caryophyllene,
473 *Atmos. Chem. Phys.*, 16, 9831-9845, 10.5194/acp-16-9831-2016, 2016a.

474 Richters, S., Herrmann, H., and Berndt, T.: Highly Oxidized RO₂ Radicals and Consecutive
475 Products from the Ozonolysis of Three Sesquiterpenes, *Environ. Sci. Technol.*, 50, 2354-2362,
476 10.1021/acs.est.5b05321, 2016b.

477 Riplinger, C. and Neese, F.: An efficient and near linear scaling pair natural orbital based local
478 coupled cluster method, *J. Chem. Phys.*, 138, 034106, 10.1063/1.4773581, 2013.

479 Shu, Y. and Atkinson, R.: Atmospheric lifetimes and fates of a series of sesquiterpenes, *J. Geophys.*
480 *Res. Atmos.*, 100, 7275-7281, <https://doi.org/10.1029/95JD00368>, 1995.

481 Taatjes, C. A., Shallcross, D. E., and Percival, C. J.: Research frontiers in the chemistry of Criegee
482 intermediates and tropospheric ozonolysis, *Phys. Chem. Chem. Phys.*, 16, 1704-1718,
483 10.1039/C3CP52842A, 2014.

484 Talukdar, R. K., Gierczak, T., McCabe, D. C., and Ravishankara, A. R.: Reaction of Hydroxyl
485 Radical with Acetone. 2. Products and Reaction Mechanism, *J. Phys. Chem. A*, 107, 5021-5032,
486 10.1021/jp0273023, 2003.

487 Vereecken, L. and Francisco, J. S.: Theoretical studies of atmospheric reaction mechanisms in the
488 troposphere, *Chemical Society Reviews*, 41, 6259-6293, 10.1039/C2CS35070J, 2012.



- 489 Weigend, F. and Ahlrichs, R.: Balanced basis sets of split valence, triple zeta valence and quadruple
490 zeta valence quality for H to Rn: Design and assessment of accuracy, *Phys. Chem. Chem. Phys.*,
491 7, 3297-3305, 10.1039/B508541A, 2005.
- 492 Weigend, F., Köhn, A., and Hättig, C.: Efficient use of the correlation consistent basis sets in
493 resolution of the identity MP2 calculations, *J. Chem. Phys.*, 116, 3175-3183, 10.1063/1.1445115,
494 2002.
- 495 Welz, O., Savee, J. D., Osborn, D. L., Vasu, S. S., Percival, C. J., Shallcross, D. E., and Taatjes, C.
496 A.: Direct Kinetic Measurements of Criegee Intermediate (CH₂OO) Formed by Reaction of CH₂I
497 with O₂, *Science*, 335, 204-207, 10.1126/science.1213229, 2012.
- 498 Winterhalter, R., Herrmann, F., Kanawati, B., Nguyen, T. L., Peeters, J., Vereecken, L., and
499 Moortgat, G. K.: The gas-phase ozonolysis of β -caryophyllene (C₁₅H₂₄). Part I: an experimental
500 study, *Phys. Chem. Chem. Phys.*, 11, 4152-4172, 10.1039/B817824K, 2009.
- 501 Wong, B. M., Matheu, D. M., and Green, W. H.: Temperature and Molecular Size Dependence of
502 the High-Pressure Limit, *J. Phys. Chem. A*, 107, 6206-6211, 10.1021/jp034165g, 2003.
- 503 Yao, L., Ma, Y., Wang, L., Zheng, J., Khalizov, A., Chen, M., Zhou, Y., Qi, L., and Cui, F.: Role of
504 stabilized Criegee Intermediate in secondary organic aerosol formation from the ozonolysis of α -
505 cedrene, *Atmos. Environ.*, 94, 448-457, <https://doi.org/10.1016/j.atmosenv.2014.05.063>, 2014.
- 506 Yao, Q., Sun, X.-H., Li, Z.-R., Chen, F.-F., and Li, X.-Y.: Pressure-Dependent Rate Rules for
507 Intramolecular H-Migration Reactions of Hydroperoxyalkylperoxy Radicals in Low Temperature,
508 *J. Phys. Chem. A*, 121, 3001-3018, 10.1021/acs.jpca.6b10818, 2017.
- 509 Yee, L. D., Isaacman-VanWertz, G., Wernis, R. A., Meng, M., Rivera, V., Kreisberg, N. M., Hering,
510 S. V., Bering, M. S., Glasius, M., Upshur, M. A., Gray Bé, A., Thomson, R. J., Geiger, F. M.,
511 Offenberg, J. H., Lewandowski, M., Kourtchev, I., Kalberer, M., de Sá, S., Martin, S. T., Alexander,



512 M. L., Palm, B. B., Hu, W., Campuzano-Jost, P., Day, D. A., Jimenez, J. L., Liu, Y., McKinney, K.
513 A., Artaxo, P., Viegas, J., Manzi, A., Oliveira, M. B., de Souza, R., Machado, L. A. T., Longo, K.,
514 and Goldstein, A. H.: Observations of sesquiterpenes and their oxidation products in central
515 Amazonia during the wet and dry seasons, *Atmos. Chem. Phys.*, 18, 10433-10457, 10.5194/acp-
516 18-10433-2018, 2018.

517 Zhao, Y. and Truhlar, D. G.: The M06 suite of density functionals for main group thermochemistry,
518 thermochemical kinetics, noncovalent interactions, excited states, and transition elements: two
519 new functionals and systematic testing of four M06-class functionals and 12 other functionals,
520 *Theor. Chem. Acc.*, 120, 215-241, 10.1007/s00214-007-0310-x, 2008.

521 Zhao, Y., Wingen, L. M., Perraud, V., and Finlayson-Pitts, B. J.: Phase, composition, and growth
522 mechanism for secondary organic aerosol from the ozonolysis of α -cedrene, *Atmos. Chem. Phys.*,
523 16, 3245-3264, 10.5194/acp-16-3245-2016, 2016.

524 Zhao, Y., Wingen, L. M., Perraud, V., Greaves, J., and Finlayson-Pitts, B. J.: Role of the reaction
525 of stabilized Criegee intermediates with peroxy radicals in particle formation and growth in air,
526 *Phys. Chem. Chem. Phys.*, 17, 12500-12514, 10.1039/C5CP01171J, 2015.

527